Vol. 4, No. 3 March 2014 ISSN 2225-7217
ARPN Journal of Science and Technology

http://www.ejournalofscience.org

Interior Solid Block Study on Combined Convection Flow through Square Enclosure with a Hot Bottom Surface

[1] M. U. Ahammad, [2] M. M. Rahman, [3] M. L. Rahman, [4] S. H. Mollah
[1, 4] Department of Mathematics, Dhaka University of Engineering and Technology (DUET), Gazipur-1700, Bangladesh
[2] Department of Mathematics, Bangladesh University of Engineering and Technology (BUET), Dhaka-1000, Bangladesh
[1, 3] Department of Mathematics, Rajshahi University, Rajshahi-6205, Bangladesh

[1] main3737@gmail.com

ABSTRACT

The combined convective flow and heat transfer of steady laminar fluids through a square enclosure with a heated bottom wall along with an interior heat conducting solid block was examined by a numerical analysis using finite element method. The effects of centered block size was studied on flow and temperature field and heat transfer performance at a particular value of Hartmann number Ha = 10, Reynolds number Re = 100 and Prandtl number Pr = 0.71 for three convective regimes of mixed convection parameter Ri (namely 0.1, 1, 10). The cavity flow patterns represented by streamlines, temperature distribution inside the cavity represented by isotherms and rate of heat transfer at the hot bottom surface represented by average Nusselt number are exposed in the present article by graphs and tables. It is seen that the internal block configuration has a significant effect on the flow and transport characteristics. The results showed that as the size of inner solid body decreases the Nusselt number increases which is very consistent with physical significance.

Keywords: *Solid block, combined convection, square enclosure, heat conduction, bottom surface*

1. INTRODUCTION

A convection situation involving both free and forced convection is commonly referred as mixed convection or combined convection. The knowledge of flow structure and heat transfer by mixed convection in a vented cavity is of interest in many physical and technological applications. Examples of combined forced and natural convection flows can be found in ventilation, solar energy storage, electronic cooling, heat rejection systems, heaters, and refrigeration devices. In this area, a large number of numerical and experimental studies have been done by many researchers. House et al. [1] studied the effect of a centered conducting body on natural convection heat transfer in an enclosure. Rahman et al. [2] performed mixed convection in a rectangular cavity having a heat-conducting horizontal circular cylinder using finite element technique. Effect of inlet and outlet position in a ventilated cavity with a heat generating square block was conducted by Ahammad et al. [3]. They presented that heat transfer at hot wall increases as Ri increases and highest heat transfer that is best cooling inside the cavity is recorded for the BB configuration. Manca et al. [4] carried out experimentally mixed convection for the assisting forced flow configuration in a channel with an open cavity. The authors found two nearly distinct fluid motions such as parallel forced flow in the channel and recirculation flow inside the cavity for a large Reynolds number (Re = 1000). A numerical investigation was carried out by Brahim and Taieb [5] to analyze the unsteady double-diffusive mixed convection in two-dimensional ventilated enclosure due to heat and contaminant sources. Steady mixed convection problem in a square enclosure that was considered differentially heated containing a rotating circular cylinder has been studied by Costa and Raimundo [6]. Angirasa [8] studied the complex interaction between natural and forced flow in a vented square enclosure with an isothermal vertical surface. The radiation effects on convective heat and mass transfer flow in a rectangular cavity was reported by Veera Suneela Rani et al [9]. In their work, Darcy model was used to analyze the combine influence of radiation and dissipation on the convective heat and mass transfer flow of a viscous fluid in a rectangular cavity through a porous medium. Khanafer et al. [10] investigated mixed convection heat transfer in two-dimensional open-ended enclosures. Chamkha [11] performed unsteady laminar mixed convection problem of electrically conducting and heat generating or absorbing fluid in a vertical lid-driven cavity in the presence of magnetic field. A numerical study of assisting MHD mixed convection inside a ventilated cavity was conducted by Sharif et al. [12]. Radhakrishnan et al. [13] revealed the outcomes of an experimental and numerical investigation of mixed convection from a heat generating element in a ventilated cavity. Parvin et al. [14] reported heat transfer enhancement by nanofluid in a cavity containing a heated obstacle. Mixed convection flows within a square cavity with uniform and non-uniform heating of bottom wall was analyzed by Basak et al. [15]. The aim of the present research is to optimize the relative size of internal solid obstacle in order to have most effective cooling in the core of the cavity by maximizing the heat-removal rate at hot wall and consequently reducing the overall temperature in the cavity.

2. PROBLEM DEFINITION

The configuration of the physical domain considered in this study is a two-dimensional ventilated cavity which is demonstrated in Fig. 1. A square solid block of diameter d is placed on the centerline of the enclosure

and this varies between 0.1L and 0.7L. A uniform homogeneous magnetic field with strength B_0 is imposed along the reverse to flow direction. The width of the cavity is equal to its length (L) and it was considered as the reference length in the dimensional analysis. The

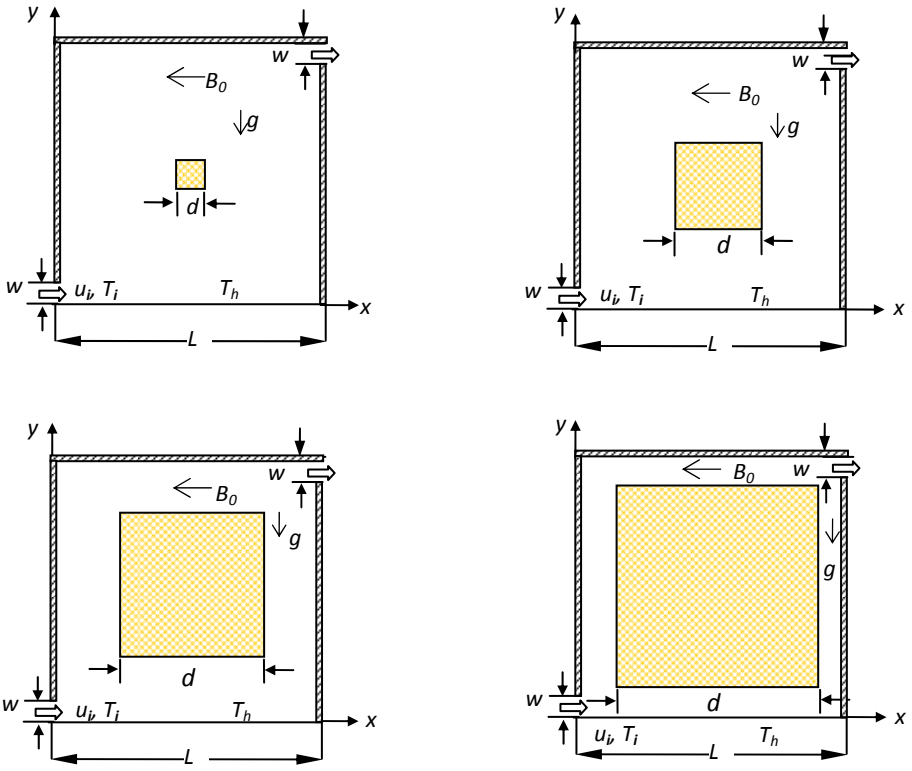

Fig 1: Studied geometry with four different centered block size

cavity's bottom wall was heated at a constant temperature and the other walls of the cavity were thermally isolated. Fresh and cold fluid is blown into the cavity via an inlet in the left side wall of the cavity while is exited through an outlet in the opposite side wall as shown in Fig. 1. In this geometry, w represents the height of the inflow and outflow openings (L/10). The no-slip condition is imposed at all the solid boundaries. The cavity fluid is assumed to be Newtonian, laminar, incompressible and steady state where all the thermo physical properties of the fluid flow were supposed to be constant. to be Newtonian, laminar, incompressible and steady state where all the thermo physical properties of the fluid flow were supposed.

Under this model, the dimensionless forms of continuity, momentum and energy equations reduce to

$$\frac{\partial u}{\partial x}+\frac{\partial v}{\partial y}=0 \tag{1}$$

$$u\frac{\partial u}{\partial x}+v\frac{\partial u}{\partial y}=-\frac{1}{\rho}\frac{\partial p}{\partial x}+\upsilon\left(\frac{\partial^2 u}{\partial x^2}+\frac{\partial^2 u}{\partial y^2}\right) \tag{2}$$

$$u\frac{\partial v}{\partial x}+v\frac{\partial v}{\partial y}=-\frac{1}{\rho}\frac{\partial p}{\partial y}+\upsilon\left(\frac{\partial^2 v}{\partial x^2}+\frac{\partial^2 v}{\partial y^2}\right)+ g\beta\left(T-T_i\right)-\sigma\frac{B_0^2 v}{\rho} \tag{3}$$

$$u\frac{\partial T}{\partial x}+v\frac{\partial T}{\partial y}=\frac{k}{\rho c_p}\left(\frac{\partial^2 T}{\partial x^2}+\frac{\partial^2 T}{\partial y^2}\right) \tag{4}$$

$$\frac{k_S}{\rho c_p}\left(\frac{\partial^2 T_s}{\partial x^2}+\frac{\partial^2 T_s}{\partial y^2}\right)=0 \tag{5}$$

where x and y are the distances measured along the horizontal and vertical directions respectively; u and v are

the velocity components in the x- and y-direction respectively; T is the temperature; ν and α are the kinematics viscosity and the thermal diffusivity respectively; p is the pressure, ρ is the density and σ is the electrical conductivity of the fluid.

2.1 Dimensional Boundary Conditions

Inlet: $u = u_i, v = 0, T = T_i$

Exit: $v = 0,\ p = 0, \dfrac{\partial T}{\partial x} = 0$

On the solid surface: $u = 0,\ v = 0$

On the bottom wall: $u = 0,\ v = 0,\ T = T_h$

On the left and right walls: $u = v = \dfrac{\partial T}{\partial x} = 0$

On the top wall: $u = v = \dfrac{\partial T}{\partial y} = 0$

At the fluid-solid interfaces: $\left(\dfrac{\partial T}{\partial n}\right)_{fluid} = \dfrac{k_s}{k}\left(\dfrac{\partial T_s}{\partial n}\right)_{solid}$

$$X = \frac{x}{L}, Y = \frac{y}{L}, D = \frac{d}{L}, U = \frac{u}{u_i}, V = \frac{v}{u_i},$$

$$P = \frac{p}{\rho\, u_i{}^2}, \theta = \frac{\left(T - T_i\right)}{\left(T_h - T_i\right)}, \theta_s = \frac{\left(T_s - T_i\right)}{\left(T_h - T_i\right)}$$

The non-dimensional variables which are given above are introduced in the equations (1-5) to obtain the non-dimensional equations (6-10) stated as:

$$\frac{\partial U}{\partial X} + \frac{\partial V}{\partial Y} = 0 \tag{6}$$

$$U\frac{\partial U}{\partial X} + V\frac{\partial U}{\partial Y} = -\frac{\partial P}{\partial X} + \frac{1}{Re}\left(\frac{\partial^2 U}{\partial X^2} + \frac{\partial^2 U}{\partial Y^2}\right) \tag{7}$$

$$U\frac{\partial V}{\partial X} + V\frac{\partial V}{\partial Y} = -\frac{\partial P}{\partial Y} + \frac{1}{Re}\left(\frac{\partial^2 V}{\partial X^2} + \frac{\partial^2 V}{\partial Y^2}\right) + \frac{Ra}{Re^2 Pr}\theta - \frac{Ha^2}{Re}V \tag{8}$$

$$U\frac{\partial \theta}{\partial X} + V\frac{\partial \theta}{\partial Y} = \frac{1}{Re\,Pr}\left(\frac{\partial^2 \theta}{\partial X^2} + \frac{\partial^2 \theta}{\partial Y^2}\right) \tag{9}$$

$$\frac{K}{RePr}\left(\frac{\partial^2 \theta_s}{\partial X^2} + \frac{\partial^2 \theta_s}{\partial Y^2}\right) = 0 \tag{10}$$

The dimensionless parameters involving the equations (6) - (10) are the Reynolds number, Rayleigh number, Prandtl number, Richardson number, Hartmann number, solid fluid thermal conductivity ratio and these are defined respectively as follows

$$Re = u_i L/\upsilon,\ Ra = g\,\beta\,\Delta T\, L^3/\upsilon\alpha,\ Pr = \upsilon/\alpha,$$
$$Ri = Gr/Re^2,\ Ha = B_0 L\sqrt{\sigma/\mu},\ K = k_s/k$$

In addition, $\Delta T = T_h - T_i$ is temperature difference and $\alpha = k/\rho c_p$ is fluid thermal diffusivity.

Non-dimensional Boundary Conditions:
Inlet:

Exit: Convective boundary condition (CBC), $P = 0$

On the solid surface: $U = 0,\ V = 0$

On the bottom wall: $U = 0,\ V = 0,\ \theta = 1$
$U = 1,\ V = 0,\ \theta = 0$

On the left and right walls: $U = V = \dfrac{\partial \theta}{\partial X} = 0$

On the top wall: $U = V = \dfrac{\partial \theta}{\partial Y} = 0$

At the fluid- solid interfaces: $\left(\dfrac{\partial \theta}{\partial N}\right)_{fluid} = K\left(\dfrac{\partial \theta_s}{\partial N}\right)_{solid}$

At the hot surface the average Nusselt number Nu is defined as $Nu_{av} = -\int_0^1 \left(\partial\theta/\partial Y\right)dX$ and the average cavity fluid temperature is $\theta_{av} = \int \theta\, d\bar{V}/\bar{V}$, $\bar{V}$ is the cavity volume.

3. NUMERICAL TECHNIQUE

The governing equations (6)-(10) of the present problem are solved numerically by finite element method along with Galerkin weighted residual technique. The procedure of solution is well described in Ahammad et al. [3] and therefore is not repeated herein.

3.1 Grid Independence

For grid refinement check five different non-uniform grid systems with 2312, 3976, 5158, 6278 and 7724 number of elements are examined in the present simulation. Table-1 shows that average Nusselt number at the hot wall and average fluid temperature in the cavity for 5158 elements gives a little difference with the corresponding outcomes for the other denser grids and thus the grid system of 5158 elements is selected for the computation of all cases for optimum results.

Table 1: Grid refinement test at Ri = 1.0, Ha = 10.0, Re = 100 and Pr = 0.71

Ele-ments	2312	3976	5158	6278	7724
Nu_{av}	5.89542	5.99234	6.02527	6.05094	6.06187
θ_{av}	0.68847	0.68985	0.69112	0.69120	0.69171

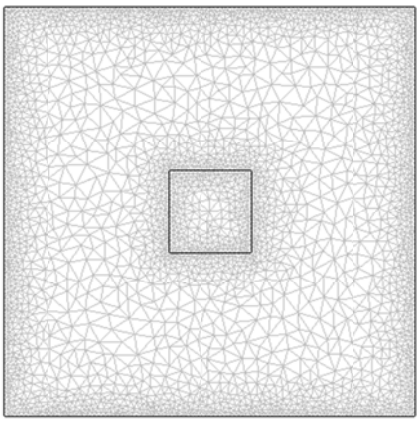

Fig 2: Grid used for the numerical simulation in the present problem

3.2 Numerical Results Validation

In order to validate the computational code, the average Nusselt numbers on the bottom heated wall obtained from the current code and those performed by House et al. [1] are tabulated in Table 2. The comparison was carried out for the Rayleigh number Ra = 0.0 and 10^5 and three values of K = 0.2, 1.0 and 5.0. House et al. [1] studied a problem of square vertical cavity of length L with a heat conducting body where the top, bottom walls were insulated and the vertical walls were isothermal and differentially heated. The mean deviations between the Nu_{av} calculated by the present simulations and those of the aforementioned study [1] were less than 1% that established the reliability of the present solver.

Table 2: Comparison of average Nusselt number with House et al.[1]

Ra	K	Nu_{av}		Error (%)
		Present study	House et al.[1]	
0	0.2	0.7082	0.7063	0.19
0	1.0	1.0001	1.0000	0.01
0	5.0	1.4153	1.4125	0.28
105	0.2	4.6228	4.6239	0.11
105	1.0	4.5041	4.5061	0.20
105	5.0	4.3187	4.3249	0.62

4. RESULTS AND DISCUSSION

The simulation on combined convection in a square cavity with centered obstacle for several cases of mixed convection parameter Ri related to different block size has been analyzed in this study. Computations are performed for four considered block configurations (D = 0.1, 0.3, 0.5, 0.7) at Re = 100, Ha = 10 and Pr = 0.71 in the range of Ri varies from 0.1 to 10 and findings are presented in terms of streamlines, isotherms, average Nusselt number at the hot wall as well as average cavity fluid temperature.

The streamline and isotherm patterns due to the variation in Richardson number are presented in Fig. 3 for solid block diameter D = 0.1. When Ri = 0.1 the open lines are found throughout the cavity and a small recirculation cell is developed at the top of the inlet port. As the Richardson number increases, the intensity of flow circulation within the cavity enhanced owing to the increase in buoyancy effect. For the largest value of Ri it can easily be noticed that the vortex swells up drastically confining the centered body so that the open streams are suppressed in the lower-right corner of the cavity which is very reasonable. In addition, for the dominant forced convection and mixed convection area it is seen that the heat lines patterns become scatter except in the vicinity of the bottom hot surface. But as the natural convection becomes dominant (Ri = 10), isotherms are found to be folded below the inner body. Also for all the considered values of Richardson number the high-isothermal lines are more concentrated near the hot wall and the temperature distribution is more uniform in the lower right parts of the cavity.

Fig. 4 shows how the behavior of the flow and thermal fields are affected under the influence of block dimension D = 0.3 in the range of Richardson number $0.1 \leq Ri \leq 10$. At Ri =0.1 the fluid streams are nearly identical with the same case for D = 0.1. On the other hand, in mixed convection area (Ri =1) it is followed that the bi-cellular vortex reduces to uni-cellular and relatively it becomes very small and so main streams spread out at the left side of the block. There is no significant change in flow characteristics for Ri =10. Close examination of the temperature field for the working domain it reveals that except a minor difference

the same is reflected in heat lines as was observed for D = 0.1.

The effects of the internal block dimension D = 0.5 at three convective regimes of Ri (0.1, 1, 10) on the streamline and isotherm patterns are displayed in Fig. 5. At Ri = 0.1 and Ri = 1, a very small eddy is created at the left side of the cavity situated above the injection port and the solid body is fully surrounded with major streams. For high value of Ri, where free convection dominates a large counter clockwise vortex is appeared that confines the obstacle. In this case open lines are seen only the bottom and right side of the cavity. The right column of Fig. 5 presents the corresponding temperature distribution. For the whole domain of Ri (0.1-10) the isotherms are clustered close to the bottom wall specially at the inlet openings, which indicates the existence of high temperature gradients in the vertical direction. Besides, thermal boundary layer is created near the hot wall and it increases in thickness slowly as Ri gets higher value.

Fig. 6 depicts the streamlines and temperature distributions for block size D = 0.7 at three selected values of Ri. From this figure it can be reported that as the value

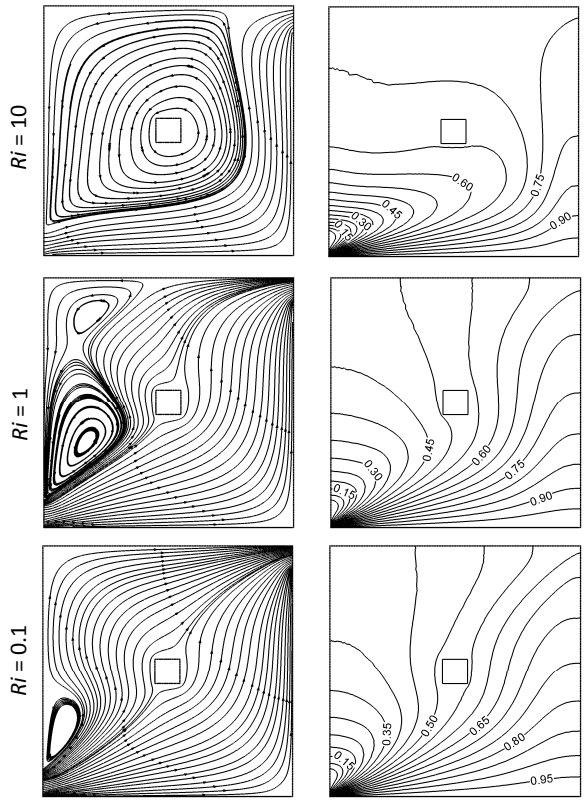

Fig 3: Streamlines (left) and Isotherms (right) in a square cavity for block diameter D = 0.1 at different values of Ri, while Re = 100, Ha = 10, Pr = 0.71

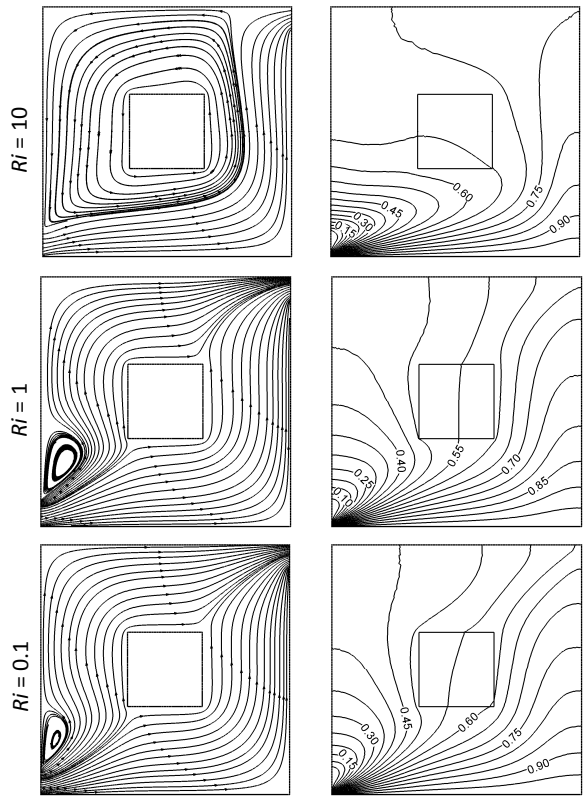

Fig 4: Streamlines (left) and Isotherms (right) in a square cavity for block diameter D = 0.3 at different values of Ri, while Re = 100, Ha = 10, Pr = 0.71

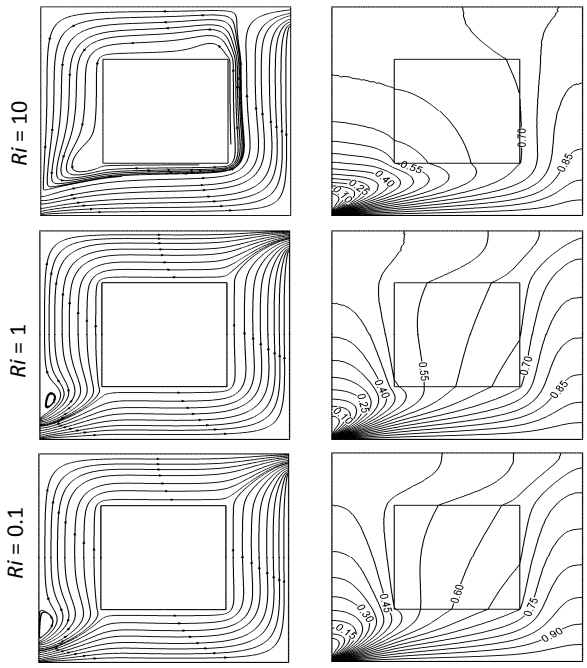

Fig 5: Streamlines (left) and Isotherms (right) in a square cavity for block diameter D = 0.5 at different values of Ri, while Re = 100, Ha = 10, Pr = 0.71

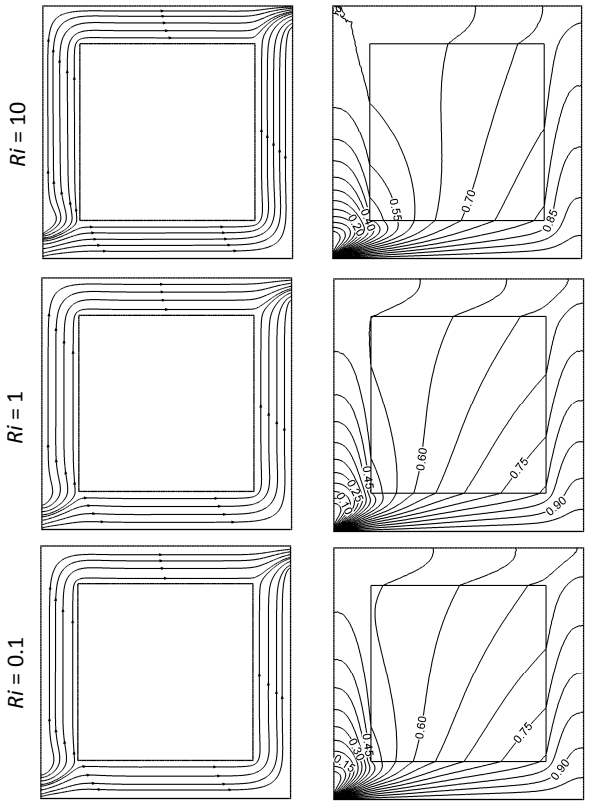

Fig 6: Streamlines (left) and Isotherms (right) in a square cavity for block diameter D = 0.7 at different values of Ri, while Re = 100, Ha = 10, Pr = 0.71

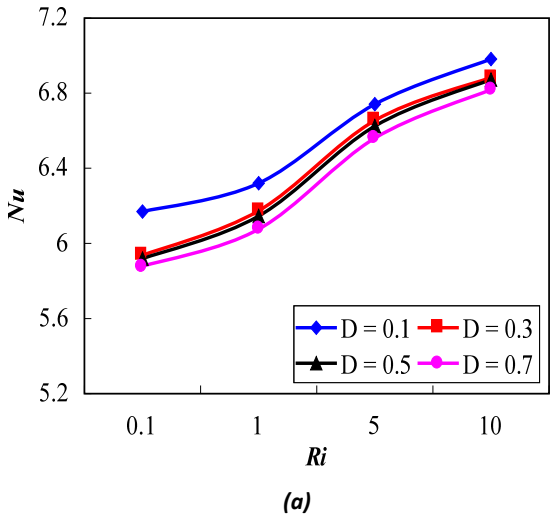

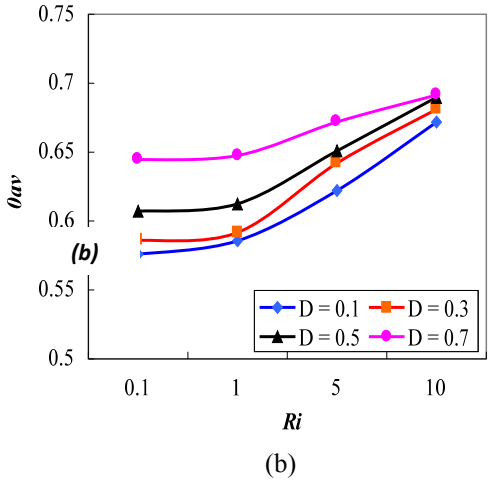

Fig 7: Effect of solid block diameter D on (a) average Nusselt number and (b) average fluid temperature in the cavity while Re = 100, Ha = 10, Pr = 0.71 and 0.1≤ Ri≤10

of D increases the vortex becomes smaller and accordingly it disappears at D = 0.7. This is the reason that for larger values of D space availability in the cavity reduces. Further, streamlines are similar in the range of 0.1 ≤ Ri ≤10 and these are found in two parts; one is bottom-right sided while the other is left-top sided of the cavity. It is noted that for all the considered values of Richardson number heat lines are distributed about uniformly over the whole cavity and these are almost similar relative to Ri.

Finally, In order to evaluate how the center lined solid block of the cavity affects the average heat transfer along the hot wall, average Nusselt number is plotted as a function of Richardson number in Fig. 7(a) for different block diameter D. This figure reveals that average Nusselt number increases rapidly with the increase of Ri. Highest heat transfer is found at the lowest value of D = 0.1 and it reduces as the value of D increases. A closer examination of Fig. 7(a) shows that there is a slight variation in average Nusselt number for the two consecutive values of D (0.3 and 0.5). On the other hand, Fig. 7(b) presents the average temperature of the fluid (θ_{av}) inside the cavity. The θ_{av} is almost invariant at low Ri (0.1≤Ri≤1) whereas it increases with higher Ri (1≤Ri≤10) for all of the preferred values of D. Another important observation is that minimum cavity fluid temperature is found for the smallest size of the block.

In addition Table 3 gives an idea about the effect of centered heat conducting block dimension in case of some selected mixed convection parameter on the average Nusselt number at the hot surface of the cavity. It is clear that as D increases Nu_{av} decreases for fixed Ri. On the other hand for a stationary value of D, Nu_{av} increases with the rising value of Ri.

Table 3: Variation of average Nusselt number (Nu_{av}) for diameter D along with Richardson number Ri

Ri	D = 0.1	D = 0.3	D = 0.5	D = 0.7
0.1	6.168909	5.936496	5.918809	5.878331
1	6.320079	6.173956	6.145851	6.075355
3	6.524987	6.347892	6.301245	6.284578
5	6.741182	6.654617	6.624877	6.560595
7	6.901246	6.792145	6.741247	6.701245
10	6.981733	6.883689	6.873435	6.819178

5. CONCLUSIONS

A two-dimensional numerical study is carried out to explain the flow patterns and heat transfer phenomena of an electrically conducting fluid subjected to externally imposed magnetic field. The flow visualization results show that in the dominant natural convection domain comparatively larger vortex is developed for the smaller block diameter D ranging from 0.1 to 0.5. The heat transfer at heated wall increases gradually as the value of D reduces with all the Richardson numbers. Last of all, it can be summarized that maximum cooling effectiveness is achieved if the dimension of the centered block is minimized.

NOMENCLATURE

B_0	magnetic induction (Wb/m2)
g	gravitational acceleration (ms-2)
h	convective heat transfer coefficient (Wm–2K–1)
Ha	Hartmann number
k	thermal conductivity of fluid (Wm-1K-1)
k_s	thermal conductivity of solid (Wm-1K-1)
L	length of the cavity (m)
Nu	Nusselt number
n	dimensional distances either x or y direction acting normal to the surface
N	non-dimensional distances either X or Y direction acting normal to the surface
p	dimensional pressure (Nm-2)
P	dimensionless pressure
Pr	Prandtl number
Ra	Rayleigh number
Re	Reynolds number
Ri	Richardson number
T	dimensional temperature (K)
ΔT	dimensional temperature difference (K)
u, v	dimensional velocity components (ms-1)
U, V	dimensionless velocity components
$\bar{V}$	cavity volume (m3)
w	height of the opening (m)
x, y	Cartesian co-ordinates (m)
X, Y	dimensionless Cartesian coordinates
α	thermal diffusivity (m2s-1)
β	thermal expansion coefficient (K-1)
ν	kinematic viscosity (m2s-1)
θ	non-dimensional temperature
ρ	density of the fluid (kgm-3)
Subscripts	
av	average
h	heated wall
i	inlet state

REFERENCES

[1] J. M. House, C. Beckermann, and T. F. Smith, "Effect of a centered conducting body on natural convection heat transfer in an enclosure," Numer. Heat Transfer, Part A, vol. 18, pp. 213-225, 1990.

[2] M. M. Rahman, M. A. Alim, and M. A.H. Mamun, "Finite element analysis of mixed convection in a rectangular cavity with a heat-conducting horizontal circular cylinder," Non-linear analysis: Modeling and Control, vol. 14, no. 2, pp. 217-247, 2009.

[3] M.U. Ahammad, M.M. Rahman, and M.L. Rahman, "Effect of inlet and outlet position in a ventilated cavity with a heat generating square block," Engineering e-Transaction, vol. 7, no. 2, pp. 107-115, 2012.

[4] O. Manca, S. Nardini, and K. Vafai, "Experimental investigation of mixed convection in a channel with an open cavity," Numerical Heat Transfer, Part A, vol. 19, pp. 53-68, 2006.

[5] Ben Beya Brahim and Lili Taieb, "Oscillatory double-diffusive mixed convection in a two-dimensional ventilated enclosure," International Journal of Heat and Mass Transfer, vol. 50, pp. 4540–4553, 2007.

[6] V. A. F. Costa and A. M. Raimundo, "Steady mixed convection in a differentially heated square enclosure with an active rotating circular cylinder," International Journal of Heat and Mass Transfer, vol. 53, pp. 1208–1219, 2010.

[7] J.N. Reddy, An Introduction to Finite Element Analysis, McGraw-Hill, New-York, 1993.

[8] D. Angirasa, "Mixed convection in a vented enclosure with an isothermal vertical surface," Fluid Dynamics Research, vol. 26, pp. 219-233, 2000.

[9] A. Veera Suneela Rani, Dr. V. Sugunamma, and N. Sandeep, "Radiation effects on convective heat and mass transfer flow in a rectangular cavity," International Journal of Innovation and Applied Studies, vol. 1, no. 1, pp. 118-152, 2012.

[10] Khalil Khanafer, Kambiz Vafai, and Marilyn Light stone, "Mixed convection heat transfer in two-dimensional open-ended enclosures," International Journal of Heat and Mass Transfer, vol. 45, pp. 5171–5190, 2002.

[11] A. J. Chamkha, "Hydro magnetic combined convection flow in a vertical lid- driven cavity with internal heat generation or absorption," Numerical Heat Transfer Part A, vol. 41, pp. 529-546, 2002.

[12] U. M. Sharif, M. M. Rahman, M. A. Saklayen, M. M. Billah, and M. Elias, "A numerical study of assisting MHD mixed convection inside a ventilated cavity," Engineering e-Transaction, vol. 7, no. 1, pp. 6–13, 2012.

[13] T.V. Radhakrishnan, A.K. Verma, C. Balaji, and S.P. Venkateshan, "An experimental and numerical investigation of mixed convection from a heat generating element in a ventilated cavity," Experimental Thermal and Fluid Science, vol. 32, pp. 502–520, 2007.

[14] S. Parvin, K. F. U. Ahmed, M. A. Alim, and N. F. Hossain, "Heat transfer enhancement by nanofluid in a cavity containing a heated obstacle," International Journal of Mechanical and Materials Engineering, vol. 7, no. 2, pp. 128-35, 2012.

[15] T. Basak, S. Roy, P.K. Sharma, and I Pop, "Analysis of mixed convection flows within a square cavity with uniform and non-uniform heating of bottom wall," Int. J. of Thermal Sci., vol. 48, no. 5, pp. 891-912, 2008.